



Synthesis, characterization, cytotoxic activity and DNA binding Ni(II) complex with the 6-hydroxy chromone-3-carbaldehyde thiosemicarbazone

Bao-dui Wang^a, Zheng-Yin Yang^{a,*}, Ming-hua Lü^b, Jun Hai^b, Qin Wang^b, Zhong-Ning Chen^c

^a College of Chemistry and Chemical Engineering and State Key Laboratory of Applied Organic Chemistry, Lanzhou University, Lanzhou 730000, PR China

^b College of life science, Lanzhou University, Lanzhou 730000, PR China

^c Fujian Institute of Research on the Structure of Matter, Chinese Academy of Sciences, Fuzhou 350002, PR China

ARTICLE INFO

Article history:

Received 8 June 2009

Received in revised form 3 August 2009

Accepted 18 August 2009

Available online 21 August 2009

Keywords:

6-hydroxy chromone-3-carbaldehyde thiosemicarbazone

Ni(II) complex

Crystal structure

DNA binding

Cytotoxic activity

ABSTRACT

A new ligand L, 6-hydroxy chromone-3-carbaldehyde thiosemicarbazone, and its Ni(II) complex have been synthesized and characterized. The crystal structure of Ni(II) complex was determined by single crystal X-ray diffraction. Ni(II) complex and ligand L were subjected to biological tests *in vitro* using THP-1, Raji and Hela cancer cell lines. Compared with the ligand, Ni(II) complex showed significant cytotoxic activity against these three cancer cell lines. The interactions of Ni(II) complex and ligand L with calf thymus DNA were then investigated by spectrometric titration, ethidium bromide displacement experiments and viscosity measurements methods. The experimental results indicated that Ni(II) complex bound to DNA by intercalative mode via the ligand L. The intrinsic binding constants of Ni(II) complex and ligand L with DNA were $(1.10 \pm 0.65) \times 10^6 \text{ M}^{-1}$ and $(1.48 \pm 0.57) \times 10^5 \text{ M}^{-1}$, respectively.

© 2009 Elsevier B.V. All rights reserved.

1. Introduction

Metal complexes of sulphur containing Schiff bases has been the subject of current and growing interest because it has been shown that many of these complexes possess anticancer activity. In particular, thiosemicarbazones, as a class of compounds, exhibit several interesting physical, chemical and wide range of biological properties [1]. Thiosemicarbazones with different chemical structures have been investigated but few works deal with chromone skeleton derivatives. Compounds containing the chromone skeleton (4H-benzopyran-4-one) (flavones and chromones) are an important class of compounds belonging to the flavonoid group that occur naturally in plants. They are minor constituents of the human diet and have been reported to exhibit a wide range of biological effects [2,3]. These biological properties include anti-inflammatory, antibacterial, antitumor [2], antioxidant [4], anti-HIV [5], vasodilator, antiviral and antiallergenic [6].

In our research, we have found that the rare earth complexes of flavane benzoyl hydrazone have certain antioxidant and cytotoxic activity, and can bind to CT-DNA by intercalation [7–9]. In view of

the above mentioned findings and as continuation of our effort to identify new potent, selective and less toxic antitumor agents, we report in the present work the synthesis of a new ligand, 6-hydroxy chromone-3-carbaldehyde thiosemicarbazone (Fig. 1), and its transition metal complex. We described a comparative study of the interactions of Ni(II) complex and ligand with CT-DNA using UV-visible, fluorescence and viscosity measurements for the first time.

2. Result and discussion

2.1. Chemistry

6-hydroxy chromone-3-carbaldehyde thiosemicarbazone was carried out by stirring the mixture of 3-formyl chromone (1) (1 mmol) with thiosemicarbazide (1 mmol) in ethanol. The progress of reaction was monitored by TLC. The resulting product was recrystallized from ethanol.

The Ni(II) complex was prepared by reacting chromone thiosemicarbazone (1 mmol) with Ni(II) nitrate (1 mmol) in ethanol. The mixtures were heated to 60 °C about 5 min, and then the mixtures was filtrated to move residue and continued stirring for 24 h at room temperature. The product was purified by washing several times with ethanol.

The structures of the synthesized compounds were determined by using spectroscopic techniques which include ¹H NMR and IR

Abbreviations: CT-DNA, calf thymus DNA; L, 6-hydroxy chromone-3-carbaldehyde thiosemicarbazone; Tris, tris(hydroxymethyl)-aminomethane; NMR, nuclear magnetic resonance; EB, ethidium bromide; CDC, 6-hydroxy-3-carboxaldehydes chromone; UV-visible, ultraviolet and visible.

* Corresponding author. Fax: +86 931 8912582.

E-mail address: yangzy@lzu.edu.cn (Z.-Y. Yang).

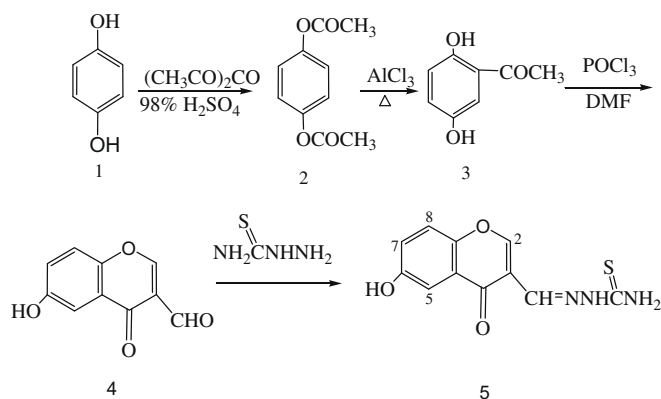


Fig. 1. Scheme of the synthesis of the ligand.

spectroscopy. The crystal structure of Ni(II) complex was determined by single crystal X-ray diffraction. Elemental analysis results were also found to be satisfactory.

2.2. IR spectra studies

The $\nu(\text{C}=\text{O})$ vibration of the free ligand is observed at 1623 cm^{-1} ; for the complex this peak high frequency shift to 1631 cm^{-1} ; $\Delta\nu_{(\text{ligand} - \text{complex})}$ is equal to 8 cm^{-1} . The band at 591 cm^{-1} is assignable to $\nu(\text{M}-\text{O})$ [10,11]. These demonstrate that the oxygen of carbonyl has formed a coordinative bond with the nickel ion. The band at 1592 cm^{-1} for the free ligand is assignable to the $\nu(\text{C}=\text{N})$ stretch [7,12], which shifts to about 1571 cm^{-1} for its complex. Weak bands at 427 cm^{-1} are assignable to $\nu(\text{M}-\text{N})$ [10,11]. These further confirm that the nitrogen of the imino-group bonds to the metal ion. Two bands at 1310 and 820 cm^{-1} are assigned to thiocarbonyl $\nu(\text{C}=\text{S})$ stretching and bending modes of vibrations [13], which are shifted towards lower energy in the spectrum of Ni(II) complex thus indicating coordination of thionato sulphur. The ν_3 (E') free nitrates appear at 1384 cm^{-1} in the spectra of the complex.

2.3. Description of the crystal structures

The structure of Ni(II) complex is shown in Fig. 2. Selected bond lengths and angles are given in Table 1. This compound crystallizes in the monoclinic $P2_1(1)/n$ space group with $Z = 4$. The structure shows that the thiosemicarbazone ligand is coordinated to nickel in the expected tridentate fashion, forming a six- and a five-membered chelate ring with O–Ni–N and N–Ni–S bite angles of $89.65(19)$ and $84.38(15)$, respectively. In Ni(II) complex, six types of Ni–ligand interactions were found. The Ni–O (3) carbonyl distances were found to be $2.033(4)\text{ \AA}$. The Ni–imine distances were found to be $2.049(5)\text{ \AA}$, for Ni–N (1). The coordinated water was found to be $2.066(5)$, $2.076(5)$ and $2.064(5)\text{ \AA}$, for Ni–O (4), Ni–O (5) and Ni–O (6), respectively.

2.4. Electronic absorption spectra

The electronic absorption peak wavelengths of ligand are 207 and 296 nm, while the Ni(II) complex presents three absorption bands at 205, 263 and 323 nm, respectively. As seen in Fig. 3, titration of CT-DNA into above Tris buffer solution containing Ni(II) complex and ligand caused some spectral changes. The absorption bands of Ni(II) complex at 205, 263 and 323 nm exhibited hypochromism of about 47, 29 and 23% and bathochromism of about 13, 3 and 2 nm, respectively. The ligand at 207 and 298 nm exhibited hypochromism of about 45% and 19% and bathochromism of

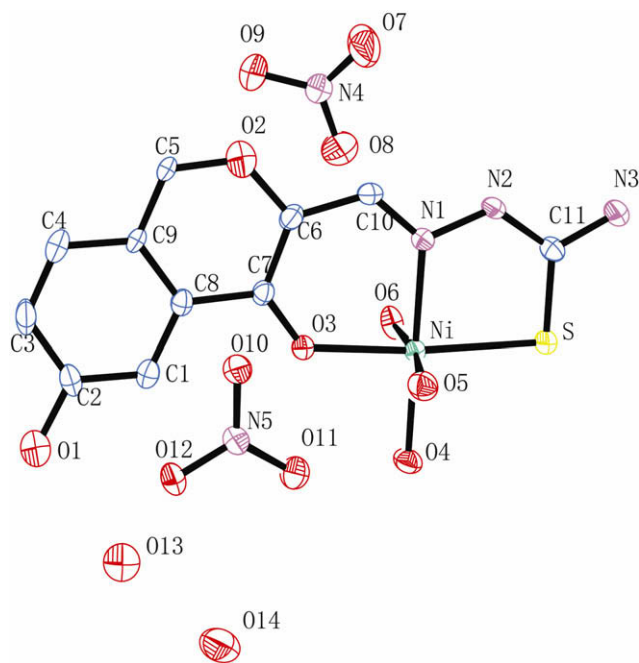


Fig. 2. The structure of complex 1.

Table 1

Select bond lengths [Å] and angles [deg] for Ni(II) complex.

Ni–O(3)	2.033(4)	O(6)–Ni–O(4)	88.6(2)
Ni–N(1)	2.049(5)	O(3)–Ni–O(5)	84.1(2)
Ni–O(6)	2.064(5)	N(1)–Ni–O(5)	92.0(2)
Ni–O(4)	2.066(5)	O(6)–Ni–O(5)	171.6(2)
Ni–O(5)	2.076(5)	O(4)–Ni–O(5)	88.5(2)
Ni–S	2.3724(18)	O(3)–Ni–S	173.78(13)
O(3)–Ni–N(1)	89.65(19)	N(1)–Ni–S	84.38(15)
O(3)–Ni–O(6)	90.9(2)	O(6)–Ni–S	93.76(15)
O(3)–Ni–O(4)	90.7(2)	O(4)–Ni–S	95.28(16)
N(1)–Ni–O(4)	179.4(2)	O(5)–Ni–S	94.

about 9 and 2 nm, respectively. Generally, large hypochromism of an aromatic dye in presence of double helical CT-DNA is characteristic of intercalation into CT-DNA base-pairs for the dye, due to the strong stacking interaction between the aromatic chromophore and the base-pairs [14,15]. So, the above phenomena imply that the Ni(II) complex and ligand interact with DNA by intercalating mode. Compared to ligand, the Ni(II) complex shows somewhat more hypochromicity, indicating that the association strength of the Ni(II) complex is much stronger than that of the free ligand.

2.5. Steady-state emission titration

The ligand and Ni(II) complex exhibit strong emission bands around 450 nm when excited at 332 nm, as shown in Fig. 5. Titration of CT-DNA led to a remarkable increase of the intensity of the emission for Ni(II) complex and ligand, as illustrated in Fig. 4. The emission behavior strongly supports that the two compounds bind to double-stranded CT-DNA by classical intercalation, because penetrating into the hydrophobic environment inside the CT-DNA can avoid the quenching effect of solvent water molecules. According to the Scatchard equation [16], a plot of r/C_f versus r gave the binding constants $(1.10 \pm 0.65) \times 10^6\text{ M}^{-1}$ and $(1.48 \pm 0.57) \times 10^5\text{ M}^{-1}$ from the fluorescence data for Ni(II) complex and ligand, respectively. These results show that the Ni(II) complex binds more strongly than the free ligand. A similar phenomenon was previously noticed to be caused by the extension of the π system of the intercalated ligand due to the coordination of the metal, such

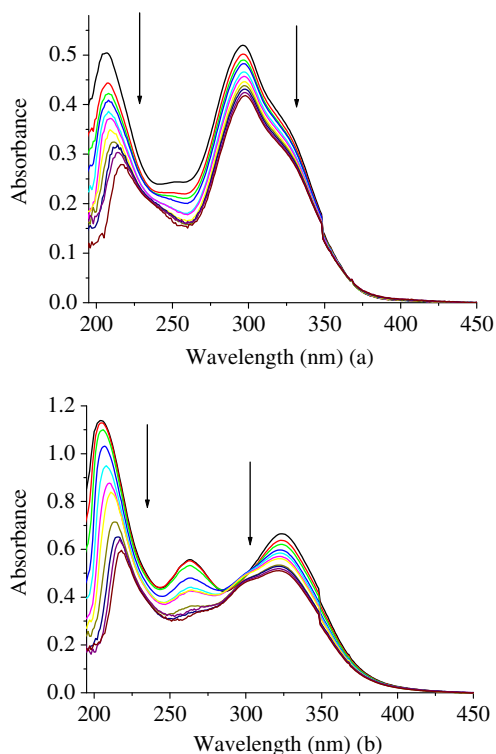


Fig. 3. (a) Electronic spectra of ligand (10 μM) in the presence of increasing amounts of CT-DNA. [DNA] = 0–25 μM . The arrow indicates the absorbance changes upon increasing DNA concentration (the concentration of DNA is expressed per nucleotide). (b) Electronic spectra of Ni(II) complex (10 μM) in the presence of increasing amounts of CT-DNA. [DNA] = 0–25 μM . The arrow indicates the absorbance changes upon increasing DNA concentration.

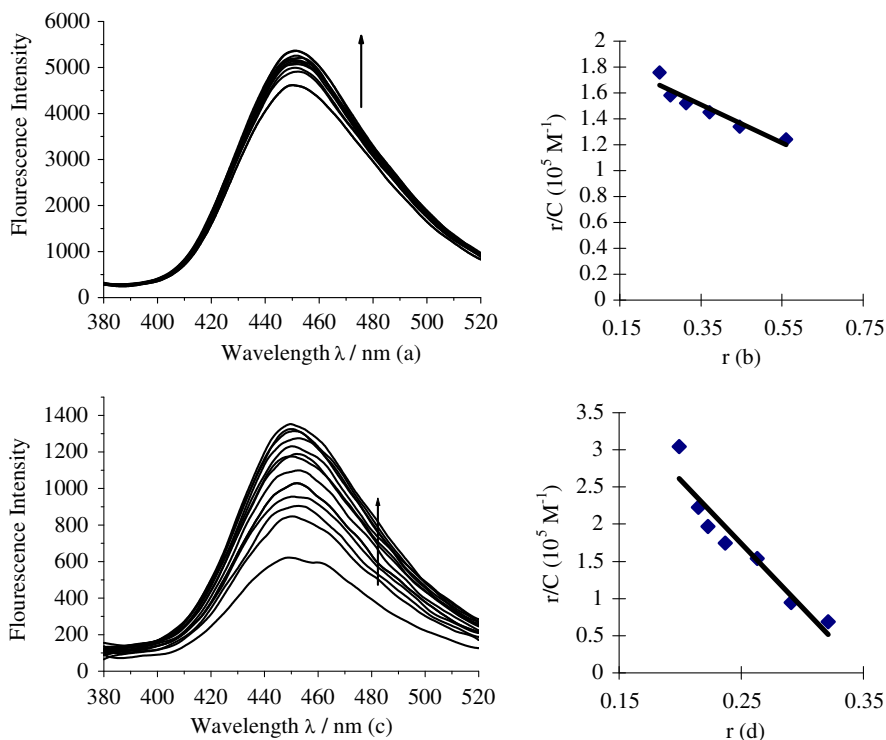


Fig. 4. (a) The emission enhancement spectra of ligand (10 μM) in the presence of 0, 2.5, 5, 7.5, 10, 12.5, 15 and 17.5 μM CT-DNA. Arrow shows the emission intensities changes upon increasing DNA concentration. Inset (b): Scatchard plot of the fluorescence titration data of ligand, $K = (1.48 \pm 0.57) 10^5 \text{ M}^{-1}$. (c) The emission enhancement spectra of Ni(II) complex (10 μM) in the presence of 0, 2.5, 5, 7.5, 10, 12.5, 15, 17.5, 20 and 22.5 μM CT-DNA. Arrow shows the emission intensities changes upon increasing DNA concentration. Inset (d): Scatchard plot of the fluorescence titration data of Ni(II) complex, $K = (1.10 \pm 0.65) \times 10^6 \text{ M}^{-1}$.

as chromone-3-carbaldehyde benzoyl hydrazone and its lanthanide complexes [7,9].

2.6. Emission quenching titration

EB is a common fluorescent probe for DNA structures and has been employed in examinations of the mode and process of metal complex binding to DNA. The fluorescent emission of EB bound to DNA in the presence of Ni(II) complex and ligand is shown in Fig. 5. The emission intensity of the DNA–EB system ($\lambda = 595 \text{ nm}$) decreased apparently as the concentration of each compound increased, which indicate that the two compounds replace EB from the DNA–EB system. The resulting decrease in fluorescence was caused by EB changing from a hydrophobic environment to an aqueous environment.

According to the classical Stern–Volmer equation [17]:

$$F_0/F = K_q[Q] + 1 \quad (1)$$

Where F_0 is the emission intensity in the absence of quencher, F is the emission intensity in the presence of quencher, K_q is the quenching constant, and $[Q]$ is the quencher concentration. The quenching plots of F_0/F vs $[Q]$ are in good agreement with the linear Stern–Volmer equation. The K_q values for the Ni(II) complex and ligand are $7.57 \times 10^3 \text{ M}^{-1}$ and $1.16 \times 10^3 \text{ M}^{-1}$, respectively.

2.7. Viscosity measurements

The interaction mode of Ni(II) complex and ligand with DNA is further confirmed via viscosity study. Intercalation is expected to increase the DNA viscosity; in contrast, a partial, nonclassical intercalation of the ligand can reduce its effective length, and concomitantly, its viscosity by bending the DNA helix [16]. In this

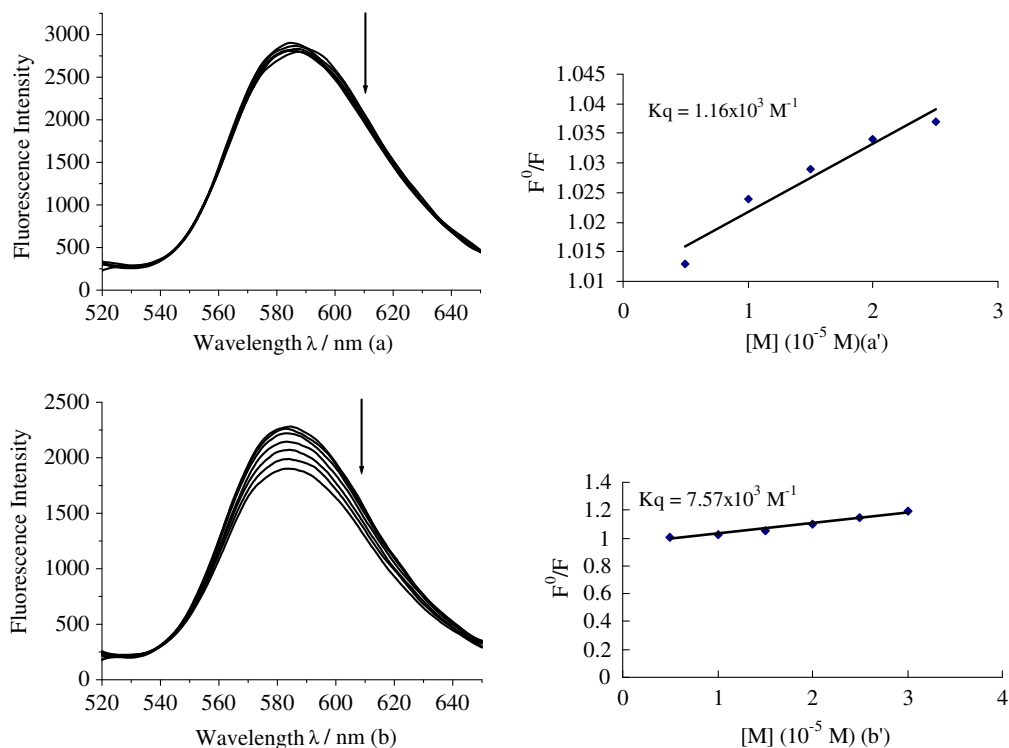


Fig. 5. (a) The emission spectra of DNA–EB system (10 M DNA and 0.32 M EB), $\lambda_{\text{ex}} = 500 \text{ nm}$, $\lambda_{\text{em}} = 520.0\text{--}650.0 \text{ nm}$, in the presence of 0, 5, 10, 15, 20, 25 M ligand. Arrow shows the emission intensities changes upon increasing ligand concentration. Inset (a'): Stern–Volmer plot of the fluorescence titration data of ligand, $Kq = 1.16 \times 10^3 \text{ M}^{-1}$. (b) The emission spectra of DNA–EB system (10 M DNA and 0.32 M EB), $\lambda_{\text{ex}} = 500 \text{ nm}$, $\lambda_{\text{em}} = 520.0\text{--}650.0 \text{ nm}$, in the presence of 0, 5, 10, 15, 20, 25 M Ni(II) complex. Arrow shows the emission intensities changes upon increasing Ni(II) complex concentration. Inset (b'): Stern–Volmer plot of the fluorescence titration data of Ni(II) complex, $Kq = 7.57 \times 10^3 \text{ M}^{-1}$.

experiment, we used the EB as a reference. As can be seen from the Fig. 6, EB can increase the relative viscosity of DNA greatly. Upon increasing the amounts of Ni(II) complex and ligand, the relative viscosity of DNA increases steadily similarly to the behavior of EB, and the extent of the viscosity increase caused by EB is more obvious. The increased degree of viscosity, which may depend on the binding affinity to DNA, follows the order of EB > Ni(II) complex > ligand. These results suggest that the binding mode of Ni(II) complex and ligand involves base-pair intercalation, and the binding affinity of Ni(II) complex is higher than that of ligand, which is consistent with the above experimental results.

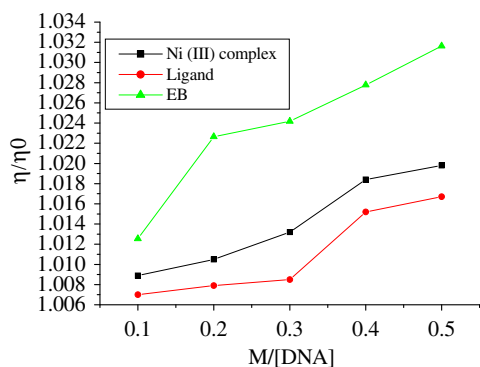


Fig. 6. Effect of increasing amounts of complexes, ligand and EB on the relative viscosity of calf thymus DNA at 25.0 °C.

2.8. Cytotoxic study

Two compounds were evaluated for their cytotoxic activity in vitro against three human cancer cell lines (THP-1, Raji and HeLa cells). The results are summarized in Figs. 7–9. The IC_{50} values of two compounds were listed in Table 2.

As shown in Figs. 7–9, the Ni(II) complex and ligand exhibited the same inhibitions on the growth of selected tumor cell lines, especially on Raji and HeLa cells in the low concentration. But the Ni(II) complex exhibited higher cytotoxic effects than that of the ligand in the high concentration. The IC_{50} values of Ni(II) complex against three cell lines were lower than that of ligand (Table 2). In the range of the tested concentration, the NiSO_4 and $\text{Ni(NO}_3)_2$ exhibited little cytotoxic activity. It is clear that the coordination of metal ion with ligand can enhance the anticancer activity of li-

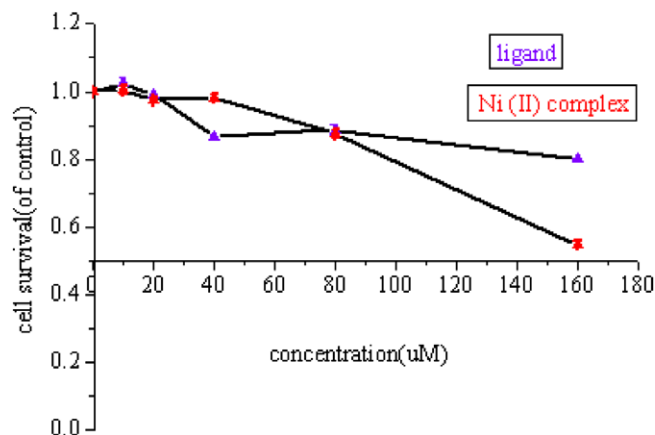


Fig. 7. Cytotoxic activity of compounds against HeLa cancer cell lines.

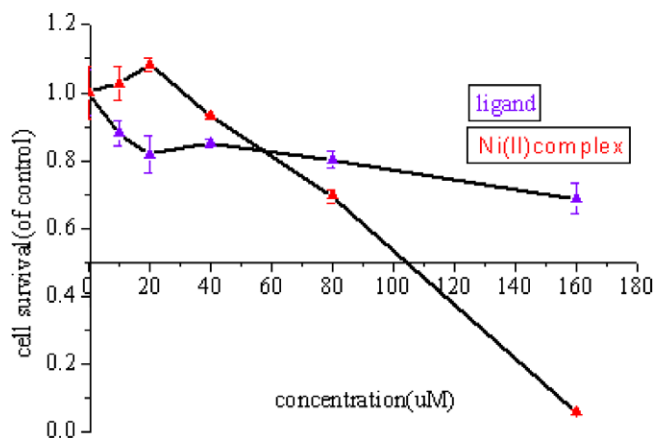


Fig. 8. Cytotoxic activity of compounds against Raji cancer cell lines.

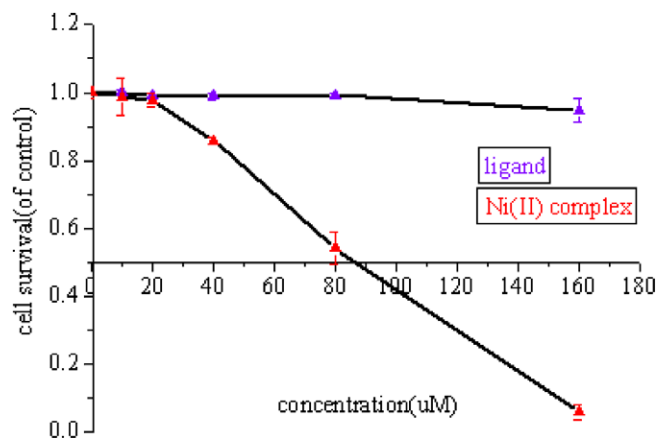


Fig. 9. Cytotoxic activity of compounds against Thp-1 cancer cell lines.

gand to the cancer cell lines. We also observed that the Ni(II) complex exhibited different cytotoxic activity in vitro against three human cancer cell lines (Hela, IC_{50} = 181 μ M; Raji, IC_{50} = 97 μ M; Thp-1, IC_{50} = 89 μ M).

2.9. Changes in cell morphological features

To validate the induction of apoptosis by identifying morphological features, phase-contrast microscopy was used to show that the dose-dependent loss in cell viability in cultures of Hela treated with ligand and Ni(II) complex was accompanied by morphological changes. Two days after treatment with Ni(II) complex, visible cell

Table 2
In vitro cytotoxicity.

	IC_{50} (μ M)		
	Type of cells	Raji	Thp-1
Ligand	>300	240.2	>300
Ni(II) complex	181	97	89

numbers decreased as Ni(II) complex concentration increased from 20 to 160 μ M. Moreover, the distinctive morphological features of cells include detachment and cell shrinkage. Hela cell death induced by Ni(II) was more obvious than ligand (Fig. 10).

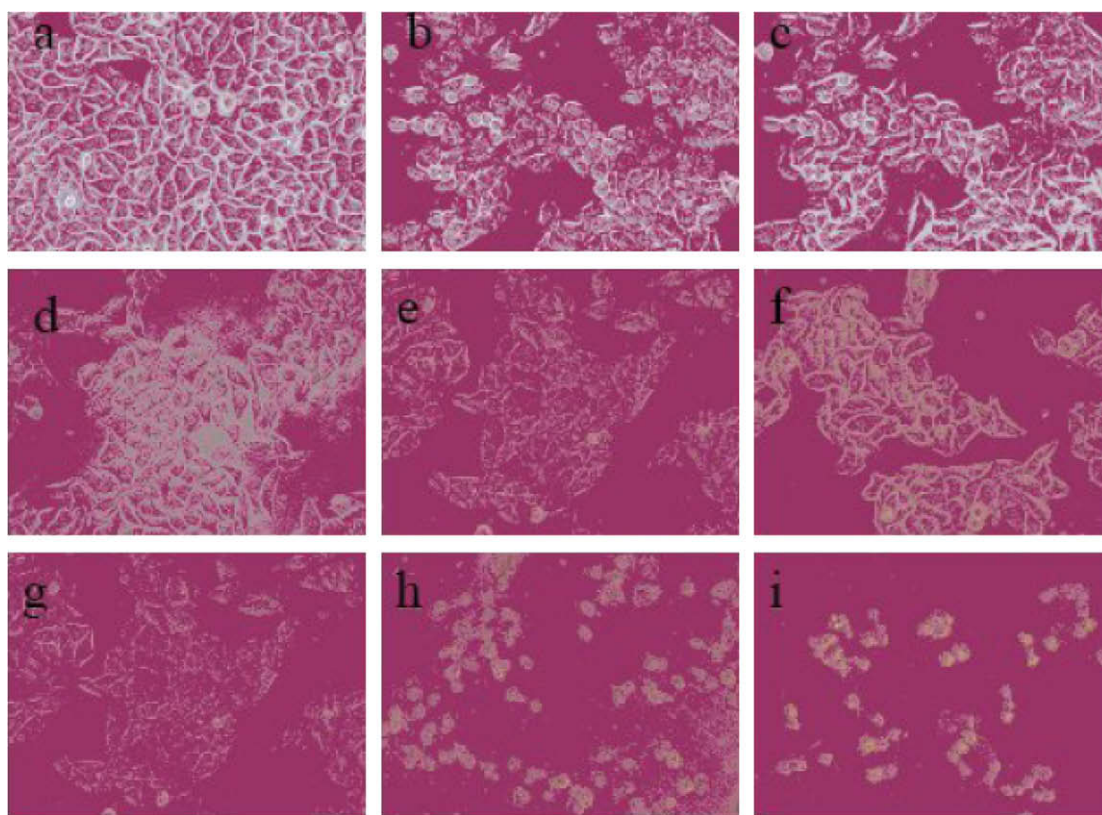


Fig. 10. Morphological characteristics of Hela cells treated with ligand or Ni(II) complex. Hela cells were seeded into tissue culture flask and treated with increasing concentrations of compounds. (a) Control, (b)–(e) 20, 40, 80 and 160 mM of ligand, (f)–(i) 20, 40, 80 and 160 mM of Ni(II) complex. Cells were photographed after 48 h drug treatment.

3. Conclusion

A novel chromone thiosemicarbazone and its Ni(II) complex were synthesized and characterized. The DNA binding mode of complex and ligand with CT-DNA were also studied via spectra and viscosity measurement. The experiment results suggest that the ligand and its complex bind to DNA via intercalation mode, and the complex has higher binding ability than free ligand. The inhibition experiment results of the complex and ligand to Hela, Raji and Thp-1 cancer cell lines suggested that the complex has high anticancer activity, and the complex has obvious selectivity against different cancer cell lines.

4. Experimental section

4.1. Chemicals

Acetic anhydride, hydroquinone and thiosemicarbazide were produced in China.

4.2. DNA sample

Calf thymus DNA (CT-DNA) was obtained from Sigma Chemicals Co. (USA) and used as received. A stock solution of CT-DNA was prepared and stored in 5 mM Tris-HCl buffer at pH 7.1. The concentration of CT-DNA solutions was determined spectrophotometrically using the reported molar absorptivity of $\epsilon_{259\text{ nm}} = 1.31 \times 10^4 \text{ M}^{-1} \text{ cm}^{-1}$ [18] and the results were expressed in terms of base-pair equivalents per cubic decimeter. A solution of CT-DNA (ca. 10^{-5} M in base-pair, bp) in Tris-HCl buffer gave a ratio of UV absorbance at 260 and 280 nm, $A_{260}/A_{280} \geq 1.9$ [19], indicating that the CT-DNA was sufficiently free from protein.

4.3. Instrumentation

Carbon, hydrogen, and nitrogen were analyzed on an Elemental Vario EL analyzer. The metal contents of the complex were determined by titration with EDTA. Infrared spectra ($4000\text{--}400 \text{ cm}^{-1}$) were determined with KBr disks on a Thermo Mattson FTIR spectrometer. The UV-visible spectra were recorded on a Varian Cary 100 Conc spectrophotometer. ^1H NMR spectra were measured on a Varian VR 300-MHz spectrometer, using TMS as a reference in DMSO- d_6 . Mass spectra were performed on a VG ZAB-HS (FAB) instrument and electrospray mass spectra (ESI-MS) were recorded on a LQC system (Finnigan MAT, USA) using CH_3OH as mobile phase. The fluorescence spectra were recorded on a Hitachi RF-4500 spectrofluorophotometer.

4.4. Preparation of ligand (L)

Organic 2 and 3 were prepared according to the literature methods [20].

The 6-hydroxy chromone-3-carbaldehyde (4): Over an ice bath, the POCl_3 (10 mL) was slowly added to a solution of 3 (1.52 g, 1 mmol) in 20 mL dry DMF. The resulting mixture was stirred at 0°C for 1 h and then at room temperature for overnight. The reaction mixture was poured into ice water. The solid was collected by vacuum filtration, washed with water, dried in vacuum, and Yield 50%. Recrystallization from 1:1 (V/V) DMF/ H_2O gave the organic 4. Yield: 50 m.p. $133\text{--}135^\circ\text{C}$. ^1H NMR (DMSO- d_6 300 MHz): δ 9.65 (1H, s, CH = O), 8.15 (1H, s, 2-H), 7.11 (1H, d, $J = 6 \text{ Hz}$, 5-H) 6.95 (1H, d, $J = 6 \text{ Hz}$, 7-H), 6.75 (1H, d, 8-H). FAB-MS: $m/z = 191[\text{M}+\text{H}]^+$.

6-hydroxy chromone-3-carbaldehyde thiosemicarbazone: An ethanol solution containing thiosemicarbazide (0.91 g, 10 mmol) was added dropwise to another ethanol solution containing 4

(1.90 g, 10 mmol). The mixture was stirred for two hours at room temperature and a yellow precipitate formed. The precipitate was collected by filtration and washed with ethanol. Recrystallization from 1:1 (V/V) DMF/ H_2O gave the ligand (L), which was dried in a vacuum. Yield: 90% m.p. $221\text{--}222^\circ\text{C}$. FAB-MS: $m/z = 264[\text{M}+\text{H}]^+$. Anal. Calc. for $\text{C}_{11}\text{H}_9\text{N}_3\text{O}_3\text{S}$: C, 50.45; H, 3.45; N, 15.96. Found: C, 50.98; H, 3.68; N, 16.08%. ^1H NMR (DMSO- d_6 300 MHz): δ 8.43 (1H, s, CH = N), 8.10 (1H, s, 2-H), 7.62 (1H, s, 5-H) 7.13 (1H, d, $J = 6 \text{ Hz}$, 7-H), 7.09 (1H, d, $J = 6 \text{ Hz}$, 8-H). IR for ligand (cm^{-1}): $\nu_{\text{C=O}}$: 1623, $\nu_{\text{C=N}}$: 1591 cm^{-1} , $\nu_{\text{C=S}}$: 1320 cm^{-1} . U_{max} (nm): 207, 296.

4.5. Preparation of complex

The ligand (1.0 mmol, 0.263 g) and the Ni(II) nitrate (1.0 mmol, 0.290 g) were added to the methanol (10 mL). The mixtures were stirred at 60°C . After 5 min, the mixtures solution was filtrated to move residue and continued stirring for 24 h at room temperature. After that, the mixtures solution was concentrated and cooled, a light blue solid separated out. The light blue precipitate was separated from the solution by suction filtration, purified by washing several times with ethanol, and dried for 24 h in a vacuum. Anal. Calc. for Ni(II) complex $\text{C}_{11}\text{H}_9\text{N}_5\text{O}_9\text{Ni}$: C, 29.35; H, 2.36; N, 15.37; Ni, 13.12. Found: C, 29.61; H, 2.02; N, 15.70; Ni, 13.16%. IR (cm^{-1}): $\nu_{\text{C=O}}$: 1631, $\nu_{\text{C=N}}$: 1571, $\nu_{\text{C=S}}$: 1168 cm^{-1} , ν_{NO_3} : 1480, 1380, 1325, 1068, 838. U_{max} (nm): 205, 264, 325.

4.6. Biological and pharmacological test

The interactions of Ni(II) complex and ligand with CT-DNA use UV-visible, fluorescence and viscosity measurements. Absorption titration experiment was performed with fixed concentrations of the drugs (10 μm) while gradually increasing concentration of CT-DNA. Viscosity experiments were conducted on an Ubbelohde viscometer, immersed in a thermostated water-bath maintained to 25°C .

Three different cell lines, uterine cervix carcinoma cell (Hela), leukemic cells (THP-1 and Raji), were plated in 96-well plates. The adherent cells, hela, was plated at a density of 5×10^4 cells/mL, nonadherent cells, THP-1 and Raji, 1×10^5 cells/mL, then treated with varied concentration (20, 40, 80, 160 and 320 μM) of the compounds. The culture medium was removed from the plates after 48 h of culture, and each well was washed once with

Table 3
Crystal data and structure refinement for Ni(II) complex.

	Ni(II) complex
Empirical formula	$\text{C}_{11} \text{H}_9 \text{N}_5 \text{Ni O}_{14} \text{S}$
Formula weight	536.08
Crystal system	Monoclinic
space group	$P2(1)/n$
a (\AA)	10.3949(2)
b (\AA)	17.13070(10)
c (\AA)	12.24160(10)
α ($^\circ$)	90
β ($^\circ$)	106.7040(10)
γ ($^\circ$)	90
V (\AA^3)	2087.90(5)
Z	4
D_{calc} (g/cm^3)	1.705
$F(000)$	1104
θ min and max ($^\circ$)	2.10–25.00
Reflections collected/unique	6839/3628 ($R(\text{int}) = 0.0264$)
Refinement method	Full-matrix least-squares on F^2
Final R indices [$I > 2\sigma(I)$]	$R1 = 0.0804$
	$wR2 = 0.2034$
R indices (all data)	$R1 = 0.0880$
	$wR2 = 0.2095$

200 μL phosphate-buffered saline (PBS, pH 7.2). To each well, 100 μL of buffer containing 0.1 M sodium acetate (pH 5.0), 0.1% Triton X-100, and 5 mM *p*-nitrophenyl phosphate (p-NPP) was added. The reaction was stopped with the addition of 10 μL of 1 M NaOH, and color development was assayed at 405 nm using a microplate reader (BIO-RAD 680). The nonenzymatic hydrolysis of the p-NPP substrate was determined for each assay by including wells that did not contain cells as blank wells. Cell survival was expressed as an absorbance (A) percentage defined by $(A_{\text{drug}} - \text{blank}) / (A_{\text{control}} - \text{blank}) \times 100$.

4.7. Crystallography

Table 3 summaries the crystal data, data collection and refinement parameters for Ni(II) complex. A light blue crystal of Ni(II) complex was determined with Bruker Smart-1000 CCD diffractometer by a graphite monochromatic Mo $K\alpha$ radiation ($\lambda = 0.71073 \text{ \AA}$) at 273(2) K. The intensity data were collected by the ω scan mode within $2.10^\circ < \theta < 25.00^\circ$ for hkl ($-11 \leq h \leq 12$, $-19 \leq k \leq 20$, $-14 \leq l \leq 11$) in the Monoclinic system. The structure was solved by direct method. The positions of rest non-Hydrogen atoms were determined from successive Fourier syntheses. The hydrogen atoms were placed in the geometrically calculated positions. H-atoms of the water molecules were not included in the structure. The positions and an isotropic thermal parameters of all non-hydrogen atoms were refined on F^2 by full-matrix least-squares techniques with SHELX-97 program package. Absorption correction was employed using Semi-empirical from equivalents.

Acknowledgement

This work is supported by the National Natural Science Foundation of China (20475023).

Appendix A. Supplementary material

Supplementary data associated with this article can be found, in the online version, at doi:10.1016/j.jorganchem.2009.08.024.

References

- [1] D.X. West, A.E. Liberta, S.B. Padhye, R.C. Chikate, P.B. Sonawane, A.S. Kumbhar, R.G. Yerande, Coordination Chemistry Reviews 123 (1993) 49.
- [2] G.W. Kabalka, A.R. Mereddy, Tetrahedron Letters 46 (2005) 6315.
- [3] S. Martens, A. Mithöfer, Phytochemistry 66 (2005) 2399.
- [4] J. Grassmann, S. Hippeli, E. Eltsner, Plant Physiology and Biochemistry 40 (2002) 471.
- [5] J. Wu, X. Wang, Y. Yic, K. Leeb, Bioorganic and Medicinal Chemistry Letters 13 (2003) 1813.
- [6] J. Seijas, M. Vázquez-Tato, R. Carballido-Reboredo, The Journal of Organic Chemistry 70 (2005) 2855.
- [7] B.D. Wang, Z.Y. Yang, P. Crewdson, D.Q. Wang, Journal of Inorganic Biochemistry 101 (2007) 1492–1504.
- [8] B.D. Wang, Z.Y. Yang, T.R. Li, Bioorganic and Medicinal Chemistry 14 (2006) 6012–6021.
- [9] B.D. Wang, Z.Y. Yang, Q. Wang, T.K. Cai, P. Crewdson, Bioorganic and Medicinal Chemistry 14 (2006) 1880–1888.
- [10] Y.Z. Yang, Synth. React. Inorg. Met.-Org. Chem. 30 (2000) 1269.
- [11] B.D. Wang, Z.Y. Yang, D.W. Zhang, Y. Wang, Spectrochim. Acta Part A 63 (2006) 213–219.
- [12] Q. Wang, Z.Y. Yang, G.F. Qi, D.D. Qin, European Journal of Medicinal Chemistry 44 (2009) 2425–2433.
- [13] L. Latheef, M.R.P. Kurup, Polyhedron 27 (2008) 35–43.
- [14] J.M. Kelly, M.J. Murphy, D.J. McConnell, C. OhUigin, Nucleic Acids Research 13 (1985) 167–184.
- [15] V.A. Bloomeld, D.M. Crothers, I. Tinico Jr. (Eds.), Physical Chemistry of Nucleic Acids, Harper and Row, 1974, p. 187.
- [16] S. Satyanarayana, J.C. Dabrowiak, J.B. Chaires, Biochemistry 31 (1992) 9319–9324.
- [17] M.R. Eftink, C.A. Ghiron, Analytical Biochemistry 114 (1981) 199–206.
- [18] J. Marmur, Journal of molecular biology 3 (1961) 208–218.
- [19] C.V. Kumar, E.H. Asuncion, Journal of American Chemical Society 115 (1993) 8547–8553.
- [20] J.X. Yu, F.M. Liu, W.J. Lu, Y.P. Li, X.M. Zao, Y.T. Liu, C. Liu, You Ji Huaxue 20 (2000) 72–80.